

Thin boron nitride nanotubes with exceptionally high strength and toughness†

Cite this: *Nanoscale*, 2013, 5, 4840

Yang Huang,^{*ab} Jing Lin,^c Jin Zou,^{*bd} Ming-Sheng Wang,^a Konstantin Faerstein,^e Chengchun Tang,^c Yoshio Bando^a and Dmitri Golberg^{*a}

Bending manipulation and direct force measurements of ultrathin boron nitride nanotubes (BNNTs) were performed inside a transmission electron microscope. Our results demonstrate an obvious transition in mechanics of BNNTs when the external diameters of nanotubes are in the range of 10 nm or less. During *in situ* transmission electron microscopy bending tests, characteristic “hollow” ripple-like structures formed in the bent ultrathin BNNTs with diameters of sub-10 nm. This peculiar buckling/bending mode makes the ultrathin BNNTs hold very high post-buckling loads which significantly exceed their initial buckling forces. Exceptional compressive/bending strength as high as ~1210 MPa was observed. Moreover, the analysis of reversible bending force curves of such ultrathin nanotubes indicates that they may store/adsorb strain energy at a density of $\sim 400 \times 10^6 \text{ J m}^{-3}$. Such nanotubes are thus very promising for strengthening and toughening of structural ceramics and may find potential applications as effective energy-absorbing materials like armor.

Received 5th February 2013

Accepted 29th March 2013

DOI: 10.1039/c3nr00651d

www.rsc.org/nanoscale

Introduction

One-dimensional nanomaterials (1D), such as nanowires and nanotubes, have attracted significant attention due to their potential applications in mechanical systems, including atomic force microscope (AFM) tips, electromechanical components and resilient composites.^{1,2} Manipulation and technological exploitation of these structures require detailed understanding of individual nanostructures. Boron nitride nanotubes (BNNTs) – one of the most intriguing non-carbon 1D nanomaterials – hold superb physical and chemical properties, *e.g.* deep ultraviolet light emission property, excellent thermal conductivity, superb thermal stability and high resistance to oxidation.^{3–9} Theoretical studies indicate that the mechanical stiffness of BNNTs can even rival that of carbon nanotubes (CNTs).^{10,11} Owing to their unique

characteristics, BNNTs are highly promising for use in composites and nanoscale optoelectronic devices working in harsh environments and at extreme temperatures.¹²

Until now, several experimental techniques have been developed for the mechanical characterization of individual BNNTs. Zettl's group studied the elastic properties of an individual cantilevered multi-walled BNNT by measuring the thermal vibration amplitude using a transmission electron microscope (TEM),¹³ from which the Young's modulus of the BNNT was found to be $1.22 \pm 0.24 \text{ TPa}$, a value comparable to that of multi-walled CNTs. Yu *et al.*¹⁴ measured the elastic modulus of BNNTs using the electric-field-induced resonance method, also using a TEM. Individual BNNTs with external diameters in the range of 34 to 94 nm displayed no strong variations in the elastic modulus, yielding an average value of 722 GPa. Later, Golberg *et al.*¹⁵ developed a direct force measurement approach to study the mechanical properties of individual BNNTs with diameters of 40–100 nm (synthesized by a CVD method using boron and metal oxide as the reactants (BOCVD)¹⁶) by virtue of an integrated TEM-AFM nano-force probing system. Through monitoring a force-deformation process for individual BNNTs during compressive bending/buckling (up to the bifurcation points) the Young's modulus of nanotubes was determined to be 0.5–0.6 TPa. Although the measurements confirmed the high stiffness of such tubes, the momentary formation of a heavily deformed kink and a sudden force drop during the compressive buckling imply that the toughness of such rather thick BNNTs is really poor.^{16–18}

Numerous studies have shown that the “effective” elasticity, strength, and plasticity of materials depend strongly upon their

^aInternational Center for Materials Nanoarchitectonics (MANA), National Institute for Materials Science (NIMS), Namiki 1-1, Tsukuba, Ibaraki 305-0044, Japan. E-mail: y.huang4@uq.edu.au; golberg.dmitri@nims.go.jp

^bSchool of Mechanical and Mining Engineering, The University of Queensland, St Lucia, QLD 4072, Australia. E-mail: j.zou@uq.edu.au

^cSchool of Material Science and Engineering, Hebei University of Technology, Tianjin 300130, P. R. China

^dCentre for Microscopy and Microanalysis, The University of Queensland, St Lucia, QLD 4072, Australia

^eNational University of Science and Technology “MISIS”, Moscow 119049, Russian Federation

† Electronic supplementary information (ESI) available: Forward and backward force-displacement curves and the corresponding TEM images of an individual BNNT (~9.5 nm in diameter) under bending deformation; and the plot of $F_{\text{max}}/F_{\text{cr}}$ with respect to the external diameters of the tested BNNTs. See DOI: 10.1039/c3nr00651d

detailed structure and chemistry. The size, shape, and “surface effects” (e.g. surface stress, roughness, and defects) of a material can significantly influence its mechanical properties, particularly when the nanometer dimensions become involved.¹⁹ A close relationship between the structure and mechanical properties also exists in 1D tubular materials.²⁰ The BNNT mechanical response could be improved by fine controlling/downsizing the tube diameters below 10 nm. Previous studies indicate that with decreasing the tube diameter, the cross-sections of BNNTs might change from characteristic polygons to nearly round shapes, and the bond angles might deviate more severely beyond the ideal sp^2 configuration, and introduce sp^3 character bonding.^{15,21,22} Thus the BNNTs with reduced diameters are expected to exhibit distinct mechanics.²³ However, to date, the mechanical behavior of ultrathin BNNTs has basically remained unknown because most of the experimental evaluations were conducted on thick BNNTs (with relatively large diameters, *ca.* >10 nm). Such a situation partially results from the technical difficulties involved in testing of such tiny objects and partially due to the lack of ideal specimens.²⁴

Very recently, we have demonstrated the large-scale preparation of BNNTs with diameters of sub-10 nm based on a modified BOCVD method,²⁵ in which a large amount of pure and thin (down to only 2-layers) BNNTs with high aspect ratios can be fabricated. In this study, we report the direct force measurements on such BNNTs and elucidate their bending properties. Our results demonstrate an obvious transition in mechanics of BNNTs when their diameter falls in the range of 10 nm or less. Such nanotubes were found to be not only stiff but also tough, possessing extremely enhanced post-buckling strength.

Experimental section

Synthesis and characterization of ultrathin BNNTs

The BNNTs were synthesized in a vertical induction furnace consisting of a fused quartz tube and an induction-heated cylindrical BN reaction chamber.²⁵ A small BN crucible, containing a mixture of Li_2O and B powders with a molar ratio of 1 : 1, was placed at the bottom of the BN reaction chamber. After evacuation of the quartz tube to $\sim 2 \times 10^{-1}$ Torr, a pure Ar flow (300 sccm) was introduced into the chamber. After the furnace was heated to ~ 1100 °C, pure NH_3 gas with a flow rate of 200 sccm was introduced. The temperature of the BN crucible was then rapidly elevated and stabilized at ~ 1350 °C, and kept constant for 3 h. The B and BO_x vapours generated during the reaction meet with NH_3 near the orifice and promote the synthesis of BN nanotubes. The grown products were directly dispersed in ethanol, dropped on a copper grid covered with a holey carbon film and analyzed using a high-resolution field-emission transmission electron microscope (TEM, JEOL, JEM-3000F) equipped with an electron energy loss spectrometer (EELS).

In situ TEM mechanical tests

The direct bending force measurements on individual nanotubes were performed using a single-tilt side-entry AFM-TEM

stage equipped with a microelectromechanical system force sensor (Nanofactory Instruments AB) using a 300 kV field-emission TEM (JEOL JEM-3100FEF) with a $2k \times 2k$ slow-scan charge coupled device (CCD) camera (for imaging and real time video-recording). To choose suitable individual BNNTs for *in situ* TEM mechanical tests, BNNTs were firstly mounted on an Al wire substrate by physically dipping the wire into the BNNT powders. The Al wire substrate was then fixed onto the AFM-TEM stage. Before the mechanical tests, the parameters of the AFM force sensor were calibrated by pushing the Al wire tip against the cantilever. The sensitivity and associated uncertainty of the force sensor was of the order of ~ 5 nN.¹⁷ During bending experiments, the carefully selected individual BNNTs, orientated nearly perpendicular to the cantilever and the Al wire substrate, were brought close to and eventually brought into contact with the Si AFM cantilever. Then the compressive bending tests were performed by further moving forward the Al substrate. The force–displacement curves were synchronically recorded and the bending processes were video-recorded in real-time using a TV-rate charge-coupled device (CCD) camera.

Results and discussion

Fig. 1a shows a bright-field TEM image of the synthesized products and shows that abundant nanotubes with high aspect ratios have been synthesized with a high purity. Fig. 1b is an enlarged TEM image and illustrates that the synthesized nanotubes are very thin. The inset is a histogram of the external diameter of the synthesized nanotubes, indicating that the majority of the nanotubes have their external diameters at 5–6 nm with many of the others having their external diameters less than 10 nm. High-resolution TEM (HRTEM) indicates that

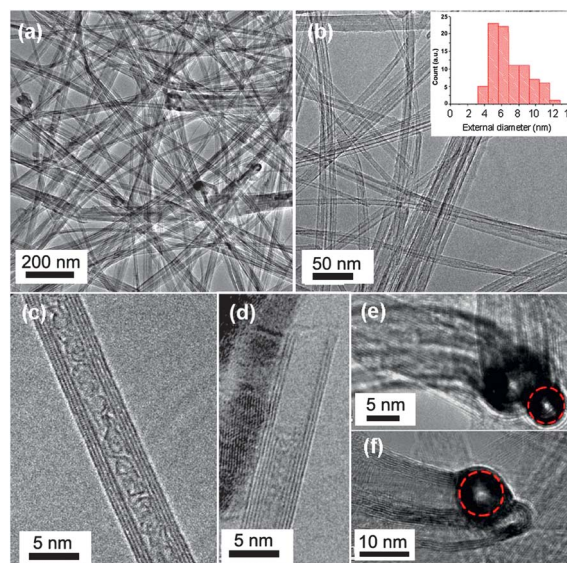


Fig. 1 (a) Low-magnification TEM image of ultrathin BNNTs product of high yield and purity. (b) Enlarged TEM images. (Inset) Histograms of the diameter distributions based on the statistics of randomly selected 90 isolated BNNTs. (c) HRTEM image of an individual four-walled BNNT. (d) TEM image of a BNNT with open tip-end. (e and f) TEM images of BNNTs with nearly round cross-sections.

the synthesized nanotubes are well-organized multi-walled structures with only a few layers. A typical BNNT with four walls is shown in Fig. 1c. The inter-wall spacing of the thin nanotube looks slightly larger than those of very thick BN tubes as well as the interlayer spacing in bulk hexagonal BN (h-BN).^{26,27} HRTEM studies also reveal that most of the synthesized nanotubes have open tip-ends, as shown in Fig. 1d–f. Since some nanotubes were orientated in parallel to the electron beam, the lateral morphology of the thin nanotubes could be directly imaged (Fig. 1e and f). These thin nanotubes demonstrate circular cross-sections, instead of polygon-like cross-sections often found in the thick multi-walled BNNTs.^{15,27}

Since the mechanical properties of any nanomaterial are sensitive to their structures and morphology, it is anticipated that our thin BNNTs should exhibit distinct mechanical properties when compared with previously reported multi-walled BNNTs with polygon-like cross-sections.¹⁶ In this regard, we carried out direct bending measurements on these thin BNNTs using the AFM-TEM stage. Based on the histogram shown in the inset of Fig. 1b, BNNTs with different diameters were synthesized, which provided us an opportunity to study the influence of tube diameter on the mechanical properties. Fig. 2a shows a straight BNNT with an external diameter of 13.5 nm clipped between the Al wire substrate and the AFM tip. When the substrate moves toward the cantilever, a compressive stress is applied to the nanotube. Once the loading force increases to a certain point, buckling/kinking of the nanotube takes place, as illustrated in Fig. 2b. Fig. 2c is an enlarged TEM image and clearly shows a localized sharp kink formed in the bent nanotube. The BN layers in the compressed side of the kink are heavily deformed, deviating from a perfect layer-by-layer stacking characteristic of the original BNNT. Particularly, the sharp kinking pattern (marked by an arrow) manifests the full existence of dislocation-like defects, *e.g.* pentagonal and heptagonal

rings in the layers. Similar behavior was also observed in multi-walled BNNTs with the external diameters of 40–100 nm.^{15,18} In contrast, for the case of BNNTs with external diameters <10 nm, distinct buckled structures and bending behaviors were observed and an example is shown in Fig. 2d–f. Fig. 2d is a typical TEM image of a thin nanotube with an external diameter of ~9.5 nm. When compressed, although the nanotube is also buckled (refer to Fig. 2e), the HRTEM image (Fig. 2f) suggests that a unique continuous ripple-like morphology forms in the compressed side of the nanotube. This morphology can be regarded as a three-ripple complex (marked by arrows in Fig. 2f). Compared with the BN layers in thicker nanotubes deformed into sharp kinks (refer to Fig. 2c), BN layers in thin nanotubes bend or deform in a comparatively mild manner, because the strain is evenly distributed between multiple ripples. As a result, the thin BNNTs can have higher tolerance to bending deformation without bond breaking or switching.

In BNNTs with even thinner diameters, the developed ripple-like structures appear to be more common and the ripples can spread over longer distances along a bent nanotube, resulting in a uniform arc morphology. Fig. 3a and b show such an example, in which a BNNT with external diameter of 5.1 nm is shown, before and during the compressive bending, respectively. The bent nanotube in Fig. 3b shows arc morphology between the substrate and the cantilever due to the formation of multiple-ripples. The ripple-like structures were also frequently observed in bent thin nanotubes during the normal TEM observations. Fig. 3c shows a BNNT with a diameter of ~8.9 nm, which contains 9 ripples. The bent BNNT has arc morphology with a bending radius of ~45 nm, indicating the flexibility of the ultrathin nanotubes.

It should be noted that the ripple-like structures were also reported in bent multi-walled CNTs (MWCNTs).^{28–32} However, the ripple characteristic observed in MWCNTs seems distinct from that observed in thin BNNTs. In the case of MWCNTs, the

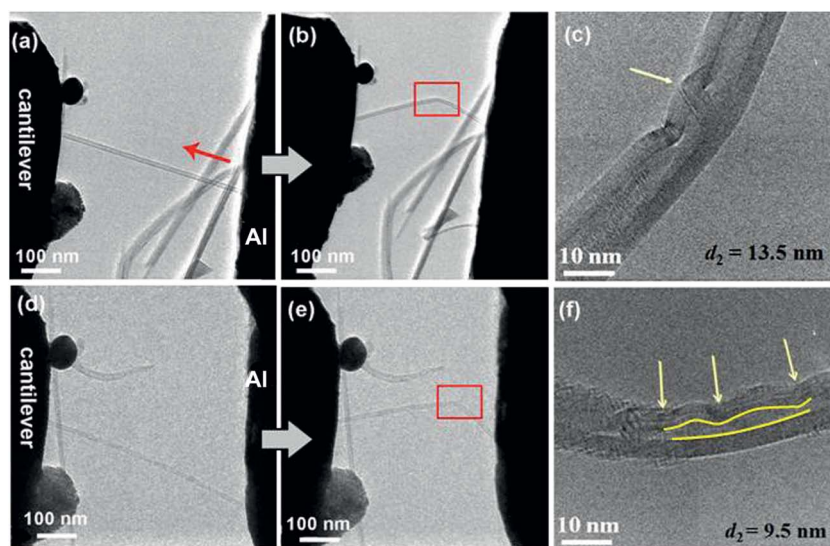


Fig. 2 (a–c) TEM images of a relatively thick BNNT with an external diameter of ~13.5 nm used for the *in situ* bending test: the starting (a) and the bent (b) states, the enlarged TEM image (c) shows heavily deformed BN layers formed at the kink. (d and e) TEM images of a representative relatively thin BNNT with an external diameter of ~9.5 nm used for the bending test. The enlarged TEM image (f) shows the three-ripple-structure in the bent nanotube.

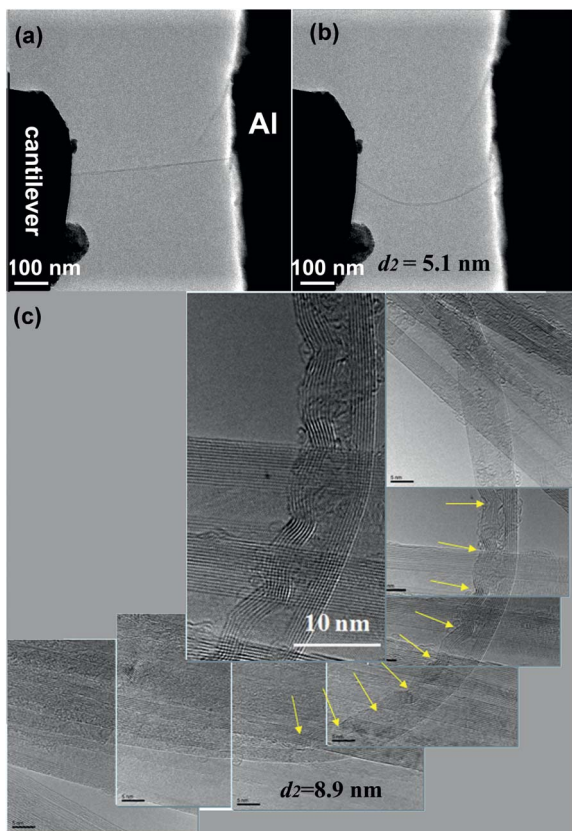


Fig. 3 (a and b) TEM images of a BNNT with an external diameter of only ~ 5.1 nm used for the *in situ* bending test under the compression load, uniform arc-like tube forms due to the prolonged ripple-like structure within the bent; (c) TEM and (inset) HRTEM images of a long rippled structure in another thin tube (external diameter ~ 8.9 nm) with a very small bending radius of ~ 45 nm.

ripple-like structures are commonly found in the thick nanotubes, of which the walls consist of tens of cylinder shells and the inner diameters are much smaller than the thicknesses of the walls; MWCNTs with large inner diameters typically form localized sharp kinks when subject to bending.³³ In addition, at the buckled segments, the diameters of inner tubes of MWCNTs often show significant reduction due to flattening, with the inner shells' distance approaching 0.35 nm, reaching the limitation where the van der Waals force becomes strongly repulsive.²⁸ In contrast, in the case of our ultrathin BNNTs, the buckled inner shells do not necessarily approach layers on the opposite stretched side during the formation of multiple-ripples. The buckled nanotubes often preserve a continuous hollow structure, as depicted in Fig. 2f and 3c. We presume that such a difference results from the partially ionic character of B–N bonds, which leads to strong so-called “lip–lip” interactions (*i.e.* interlayer coupling) between adjacent layers. As a result, a BNNT wall constructed of multi-layers behaves as quasi-continuum matter. That is distinct from MWCNTs, where each tube layer can slide easily one upon another when a deformation takes place.^{34,35} The capability of keeping hollow tubes during the compression-induced bending indicates that the present thin BNNTs can possess higher bending stiffness than CNTs of similar geometry.

The above analysis indicates that the BNNTs with various diameters show different buckling/bending modes, which can also be reflected in their force–displacement (F – d) curves. Fig. 4a–c show the forward F – d curves measured for the above-mentioned BNNTs with external diameters of ~ 13.5 nm, ~ 9.5 nm and ~ 5.1 nm, respectively. These curves confirm a mechanical response transformation within this diameter range.

In the case of a relatively thick BNNT (refer to the BNNT shown in Fig. 2a–c), with increasing the displacement, the measured force increases near linearly to a maximum value (F_{\max}) of 42 nN, then declines quickly with a force drop of more than 50% and finally remains at a stable value (~ 20 nN) with minor variations. It has been suggested that for a long straight column subjected to the compressive stress, the critical load (F_{cr}), which causes the column to fail by buckling, can be estimated by the Euler formula $F_{\text{cr}} = \pi^2 EI/L^2$, where E is the Young's modulus, I is the moment of inertia: $I = \pi(d_2^4 - d_1^4)/64$, where d_2 and d_1 are the external and internal diameters of the nanotube, respectively, and L is the tube length between two contacts.^{1,15} Based on the commonly used Young's modulus of the thin BNNT of ~ 0.8 TPa,¹⁴ the critical load of the nanotube

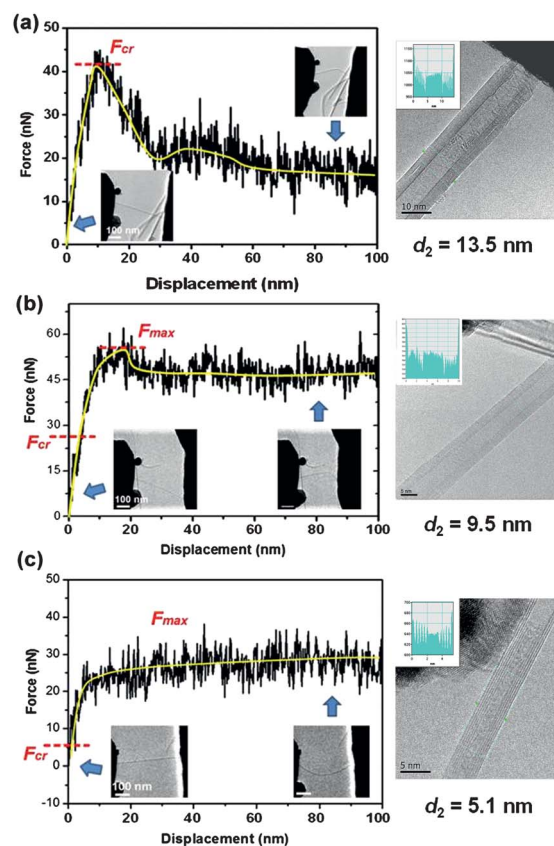


Fig. 4 (a) Force measurements under bending of a relatively thick BNNT with an external diameter of ~ 13.5 nm: (left) force–displacement curve; (right) HRTEM image of the BNNT. (b and c) Force measurements under bending of typical BNNTs with diameters of sub-10 nm: (b) force–displacement curve (left) of a BNNT with an external diameter of ~ 9.5 nm and the corresponding HRTEM image (right); (c) force–displacement curve (left) of an ultrathin BNNT with an external diameter of ~ 5 nm and the corresponding HRTEM image (right).

can be estimated to be ~ 46 nN. We note that this value agrees well with the maximum axial load (aF_{\max}), which can be calculated using $aF_{\max} = F_{\max}/\cos \theta$. Since angle θ between the tube axis and the trace of cantilever deflection is small, $aF_{\max} \approx F_{\max}$.^{36,37} This indicates that the tested BNNT indeed loses its load-carrying capacity at the moment of Euler buckling. The sudden drop in loading force results from a structural failure of the BNNT. Similar phenomena were also observed in the BNNTs prepared *via* the BOCVD method,^{15,18} although in that case the force dropped more abruptly. Fast propagation of defects in a localized kink is believed to cause sudden stress release in such BNNTs. This process is accompanied by breakage of numerous B–N bonds, distortion and instantaneous rearrangement. Using the diameter measured under HRTEM, the axial compressive/bending strength ($\sigma = (F_{\max}/\cos \theta)/S$, where S is the area of the tube cross-section) can be determined to be ~ 300 MPa.

The F – d curves measured for the thinner BNNT (refer to the BNNT shown in Fig. 2d–f) also show that the measured force declines after a maximum of ~ 52 nN is reached. The force finally stabilizes at ~ 45 nN; the overall force loss is about 10%. Another feature is that the force curve apparently deviates from the linearity before reaching the maximum. Using the Euler formula and the Young's modulus of ~ 0.8 TPa for the BNNT, we estimate that the present thinner BNNT should be buckled under a critical load (F_{cr}) of ~ 12 nN. This value is much smaller than the estimated aF_{\max} of ~ 55 nN. Apparently, the thinner BNNT holds very high post-buckling force, significantly in excess of its initial buckling load (more than 4 times),³⁸ indicating that the thinner BNNT can have greatly enhanced axial carrying capacity. We attribute the strengthening in the thinner BNNTs to the formation of the unique ripple-like structures. When the applied load increases beyond the critical load, thin BNNTs buckle. Continuous compression makes the nanotubes deviate from their original straight configuration, while the ripples allow such deviations to take place through numerous B–N bond stretching/bending without breakage. As a result, the force increases nonlinearly. Once the force exceeds F_{\max} , the accumulated stress causes partial B–N bond breaking at certain ripples and in turn leads to a slight force decrease. At this point, the nanotube still retains a nearly straight geometry, as evidenced by video-recording (see ESI, Fig. S1†) and a negligible compressive displacement (~ 18 nm) compared to the entire length (~ 500 nm) of the nanotube. This is consistent with TEM results that thin BNNTs tend to form “hollow” ripple-structures. The buckling/bending mode involving a following-up strengthening process and characteristically high F_{\max} values implies that the ultrathin BNNTs possess both superb toughness and stiffness. In fact, the present thinner nanotube holds an exceptionally high compressive/bending strength of ~ 880 MPa.

For the thinnest nanotube ($d_2 = \sim 5$ nm, refer to the BNNT shown in Fig. 3a and b), no notable force drop was detected during the entire bending process. The measured force increases quickly within the initial displacement, up to ~ 20 nm, and then increases gradually, approaching the maximum of ~ 30 nN. Herein, the maximum axial load ($aF_{\max} \approx F_{\max}/\cos \theta$, as the nanotube is still nearly straight at this

moment) on the nanotube is also much higher (>6 times) than the critical buckling load (~ 5 nN) estimated using the Euler formula, and points at the super-high axial compressive/bending strength of ~ 1210 MPa. Similarly, the continuous force increase is attributed here to the formation of long ripple-like structure with only trace amounts of B–N bonds broken. The results of force measurements on the BNNTs of different diameters show that post-buckling strengthening is common and peculiar to ultrathin BNNTs, but rare in comparatively thick BNNTs (see ESI, Fig. S2†). Therefore, we can conclude that the ultrathin BNNTs with diameters of less than 10 nm can be not only stiff but also tough, possessing a very high ultimate bending strength.

The structural reversibility under bending of BNNTs and/or CNTs has been widely studied previously as evidence of their excellent flexibility.^{15,20} In our experiments, the BNNTs were bent to more than 70° . Once the load was removed, the nanotubes could completely restore their original shapes (Fig. 5a and ESI, Fig. S1†). We thoroughly analyzed the recovery process *via* measuring the forward–backward F – d curves of the ultrathin BNNTs, as shown in Fig. 5b. The curves show overlapped forward–backward plots, indicating that the buckles and bents are entirely elastic. Thus the work done by the forward loading force generates the elastic energy which is stored in the ultrathin BNNTs and can be released during the backward movement. By integrating the experimental F – d curves,³⁹ we can approximately estimate the recoverable energy in the presently bent BNNT to be $\sim 400 \times 10^6$ J m^{−3}. For a comparison, a CNT spring made of bundles of single-walled CNTs stretched to a 10% strain has been predicted to possess the stored energy of 3.4×10^6 kJ m^{−3}.⁴⁰ For the thicker BNNTs, the energy may be dissipated *via* bond breakage or rearrangement, as a result, the recoverable energy (per volume) should be much less than that of the thinner BNNTs. Therefore, the capability of thin BNNTs to elastically sustain large loads makes them attractive materials to store and/or absorb considerable strain energy.

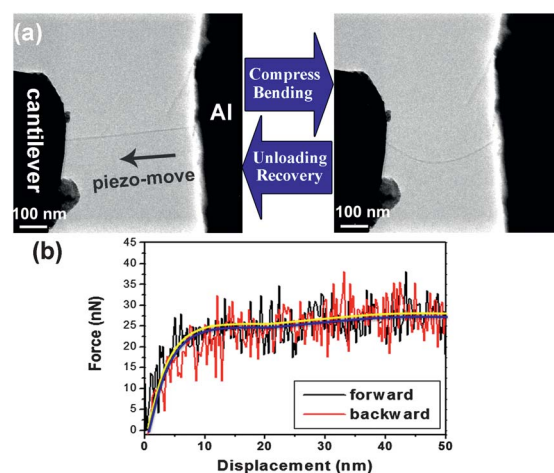


Fig. 5 (a) Reversible bending deformation of an ultrathin BNNT and (b) forward–backward force–displacement curves.

Conclusions

In summary, direct bending experiments were performed on the BNNTs synthesized by the modified BOCVD method. A distinct mechanical response was found in thin BNNTs with diameters less than 10 nm. During *in situ* TEM bending tests, heavily deformed BN layers formed in thick BNNTs, while characteristic “hollow” ripple-like structures formed in the bent ultrathin BNNTs. This peculiar buckling/bending mode makes the ultrathin BNNTs possess very high post-buckling loads which significantly exceed their initial buckling forces. The exceptional compressive/bending strength of ~ 1210 MPa was observed. Moreover, the analysis of reversible bending force curves of such ultrathin tubes indicates that they may store/adsorb strain energy at a density of $\sim 400 \times 10^6$ J m $^{-3}$. Such nanotubes with excellent mechanical performance combined with other superb physical and chemical properties are thus very promising for strengthening and toughening of structural ceramics and may find potential applications as effective energy-absorbing materials like armor.

Acknowledgements

This work was financially supported in part by the UQ New Staff Research Start-Up Funds, UQ Early Career Research Grants, Australian Research Council, World Premier International (WPI) Center for Materials Nanoarchitectonics (MANA) of the National Institute for Materials Science (NIMS), National Natural Science Foundation of China (Grant no. 51202055, no. 21103056 and no. 10974041), Natural Science Foundation of Hebei Province (Grant no. E2012202040), the Innovation Fund for Excellent Youth of Hebei University of Technology (no.2012001), a Grant-in-Aid no. 23310082 (JSPS, Japan) and a Grant of Russian Federation Ministry for Science and Education (agreement no. 11.G34.31.0061).

References

- H. Dai, J. H. Hafner, A. G. Rinzler, D. T. Colber and R. E. Smalley, *Nature*, 1996, **384**, 147.
- J. N. Coleman, U. Khan and Y. K. Gun'ko, *Adv. Mater.*, 2006, **18**, 689.
- A. Rubio, J. L. Corkill and M. L. Cohen, *Phys. Rev. B: Condens. Matter Mater. Phys.*, 1994, **49**, 5081.
- N. G. Chopra, R. J. Luyken, K. Cherrey, V. H. Crespi, M. L. Cohen, S. G. Louie and A. Zettl, *Science*, 1995, **269**, 966.
- X. Blase, A. Rubio, S. G. Louie and M. L. Cohen, *Europhys. Lett.*, 1994, **28**, 335.
- D. Golberg, Y. Bando, C. Tang and C. Zhi, *Adv. Mater.*, 2007, **19**, 2413.
- L. H. Li, Y. Chen, M. Lin, A. M. Glushenkov, B. Cheng and J. Yu, *Appl. Phys. Lett.*, 2010, **97**, 141104.
- C. Y. Zhi, Y. Bando, C. Tang, D. Golberg, R. Xie and T. Sekiguchi, *Appl. Phys. Lett.*, 2005, **86**, 213110.
- P. Kim, L. Shi, A. Majumdar and P. L. McEuen, *Phys. Rev. Lett.*, 2001, **87**, 215502.
- E. Hernandez, C. Goze, P. Bernier and A. Rubio, *Phys. Rev. Lett.*, 1998, **80**, 4502.
- K. N. Kudin, G. E. Scuseria and B. I. Yakobson, *Phys. Rev. B: Condens. Matter Mater. Phys.*, 2001, **64**, 235406.
- R. B. Patela, J. Liu, J. Eng and Z. Iqbal, *J. Mater. Res.*, 2011, **26**, 1332; M. Yamaguchi, A. Pakdel, C. Zhi, Y. Bando, D. Tang, K. Faerstein, D. Shtansky and D. Golberg, *Nanoscale Res. Lett.*, 2013, **8**, 3.
- N. G. Chopra and A. Zettl, *Solid State Commun.*, 1998, **105**, 297.
- A. P. Suryavanshi, M. Yu, J. Wen, C. Tang and Y. Bando, *Appl. Phys. Lett.*, 2004, **84**, 2527.
- D. Golberg, P. M. F. J. Costa, O. Lourie, M. Mitome, X. Bai, K. Kurashima, C. Zhi, C. Tang and Y. Bando, *Nano Lett.*, 2007, **7**, 2146.
- C. C. Tang, Y. Bando, T. Sato and K. Kurashima, *Chem. Commun.*, 2002, 1290.
- D. Golberg, P. M. F. J. Costa, M. Wang, X. Wei, D. Tang, Z. Xu, Y. Huang, U. K. Gautam, B. Liu, H. Zeng, N. Kawamoto, C. Zhi, M. Mitome and Y. Bando, *Adv. Mater.*, 2012, **24**, 177.
- H. M. Ghassemi, C. H. Lee, Y. K. Yap and R. S. Yassar, *J. Appl. Phys.*, 2010, **108**, 024314.
- M. J. Gordon, T. Baron, F. Dhalluin, P. Gentile and P. Ferret, *Nano Lett.*, 2009, **9**, 525.
- M. R. Falvo, G. J. Clary, R. M. Taylor, V. Vhi, F. P. Brooks Jr, S. Washburn and R. Superfine, *Nature*, 1997, **389**, 582.
- C. H. Kiang, M. Endo, P. M. Ajayan, G. Dresselhaus and M. S. Dresselhaus, *Phys. Rev. Lett.*, 1998, **81**, 1869; Y. Gogotsi, *Nanotubes and Nanofibers*, Taylor & Francis, USA, 2006, ch. 3.
- D. Golberg, M. Mitome, Y. Bando, C. C. Tang and C. Y. Zhi, *Appl. Phys. A*, 2007, **88**, 347.
- J. Garel, I. Leven, C. Y. Zhi, K. S. Nagapriya, R. Popovitz-Biro, D. Golberg, Y. Bando, O. Hod and E. Joselevich, *Nano Lett.*, 2012, **12**, 6347.
- R. Arenal, M. S. Wang, Z. Xu, A. Loiseau and D. Golberg, *Nanotechnology*, 2011, **22**, 265704.
- Y. Huang, J. Lin, C. Tang, Y. Bando, C. Zhi, T. Zhai, B. Dierre, T. Sekiguchi and D. Golberg, *Nanotechnology*, 2011, **22**, 145602.
- Y. Huang, Y. Bando, C. Tang, C. Zhi, T. Terao, B. Dierre, T. Sekiguchi and D. Golberg, *Nanotechnology*, 2009, **20**, 085705.
- A. Celik-Aktas, J. M. Zuo, J. F. Stubbins, C. Tang and Y. Bando, *Acta Crystallogr., Sect. A: Found. Crystallogr.*, 2005, **61**, 533.
- S. Iijima, C. Brabec, A. Maiti and J. Bernholc, *J. Chem. Phys.*, 1996, **104**, 2089.
- T. Kuzumaki, T. Hayashi, H. Ichinose, K. Miyazawa, K. Ito and Y. Ishida, *Philos. Mag. A*, 1998, **77**, 1461.
- P. Poncharal, Z. L. Wang, D. Ugarte and W. A. Heer, *Science*, 1999, **283**, 1513.
- M. F. Yu, O. Lourie, J. Dyer, K. Moloni, T. F. Kelly and R. S. Ruoff, *Science*, 2000, **287**, 637.
- O. Lourie, D. M. Cox and H. D. Wagner, *Phys. Rev. Lett.*, 1998, **81**, 1638.

- 33 M. Arroyo and I. Arias, *J. Mech. Phys. Solids*, 2008, **56**, 1224; A. Sears and R. C. Batra, *Phys. Rev. B: Condens. Matter Mater. Phys.*, 2006, **73**, 985410.
- 34 J. Cumings and A. Zettl, *Science*, 2000, **289**, 602.
- 35 A. N. Kolmogorov and V. H. Crespi, *Phys. Rev. Lett.*, 2000, **85**, 4727.
- 36 X. L. Wei, M. S. Wang, Y. Bando and D. Golberg, *Adv. Mater.*, 2010, **22**, 4895.
- 37 D. M. Tang, C. L. Ren, M. S. Wang, X. L. Wei, N. Kawamoto, C. Liu, Y. Bando, M. Mitome, N. Fukata and D. Golberg, *Nano Lett.*, 2012, **12**, 1898.
- 38 G. J. Simitzes, *Appl. Mech. Rev.*, 1986, **39**, 1517.
- 39 E. W. Wong, P. E. Sheehan and C. M. Lieber, *Science*, 1997, **277**, 1971.
- 40 F. A. Hill, T. F. Havel and C. Livermore, *Nanotechnology*, 2009, **20**, 255794.